Supporting Information

Hovering spreading rebound on porous superhydrophobic surface with active air plastron for rapid drop detachment

Yatong Wang,[#a] Bingzhe Xu,[#a] Zhen Chen,[b] Guohao Li [a], and Zhe Li[*a]

[a]Guangdong Provincial Key Laboratory of Sensor Technology and Biomedical Instrument, School of Biomedical Engineering, Sun Yat-Sen University, Guangzhou 510006, China.

[b]School of Naval Architecture, Ocean and Civil Engineering, Shanghai Jiao Tong University, Shanghai 200240, China.

[#] These authors contribute equally.

[*] Corresponding author: Prof. Zhe Li; E-mail: lizhe28@mail.sysu.edu.cn

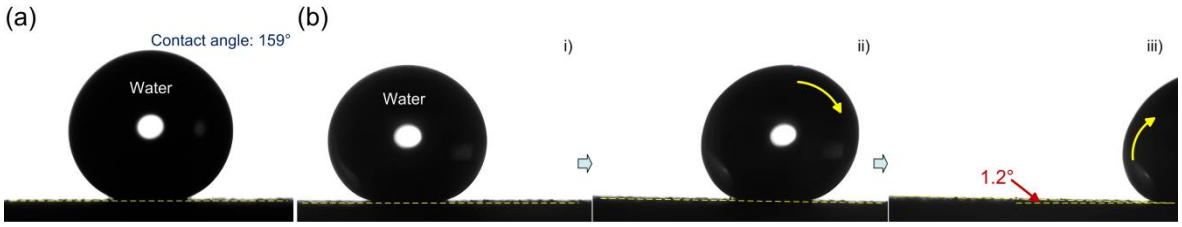

Fig. S1. Water contact angle and roll-off angle of the porous superhydrophobic surface. (A) A 5 µl water drop sitting on the surface, showing a contact angle of 159 °. (B) A 10 µl water drop rolling off the surface at a small inclination angle of 1.2 °.

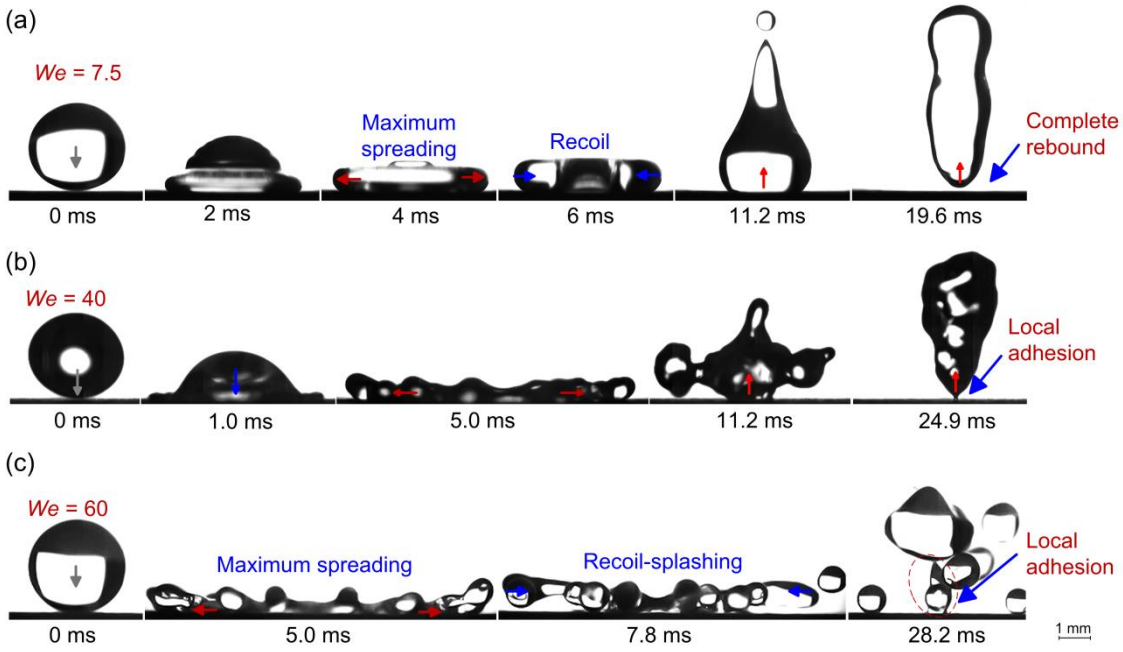

Fig. S2. Water drops impacting on the passive porous superhydrophobic surface without active air plastron (P = 0 kPa). (a) We = 7.5; complete rebound occurred at 19.6 ms; (b) We = 40; partial rebound was observed at 24.9 ms; (c) We = 60; recoil-splashing occurred at 7.8 ms and drop adhesion was observed at 28.2 ms. Diameter of the water drop: 3.04 mm.

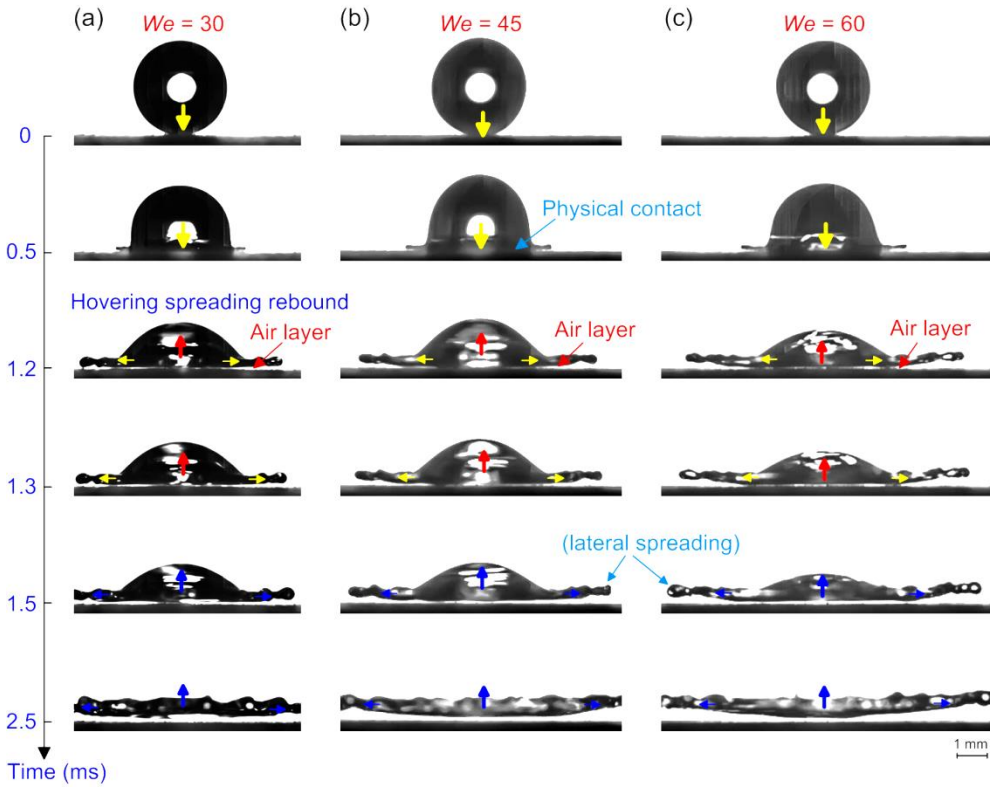

Fig. S3. Hovering spreading rebound of water drops impacting on the porous superhydrophobic surface with high pressure active air plastron (P = 200 kPa). (a) We = 30, (b) We = 45 and (c) We = 60. Hovering spreading rebound was observed to occur around 1.2 ms, with a thin layer of air plastron formed beneath the impacting drop. After rebound, the drop continued to spread while hovering in the air. Diameter of the water drop: 3.04 mm.

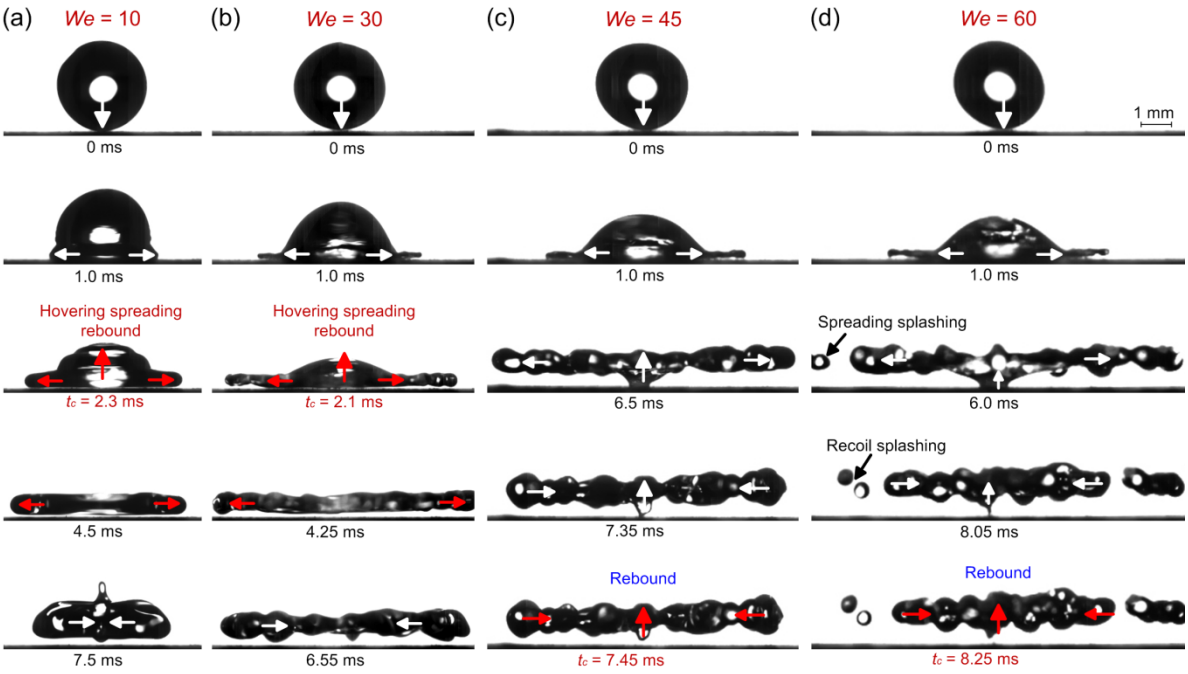

Fig. S4. Water drops impacting on the porous superhydrophobic surface with low pressure active air plastron (P = 100 kPa). (a) We = 10, (b) We = 30, (c) We = 45 and (d) We = 60. Hovering spreading rebound occurred at We = 10 or 30; the contact time at We = 10 and 30 is 2.3 ms and 2.1 ms, respectively. At high Weber numbers (We = 45 or 60), hovering rebound did not occur. Diameter of the water drop: 3.04 mm.

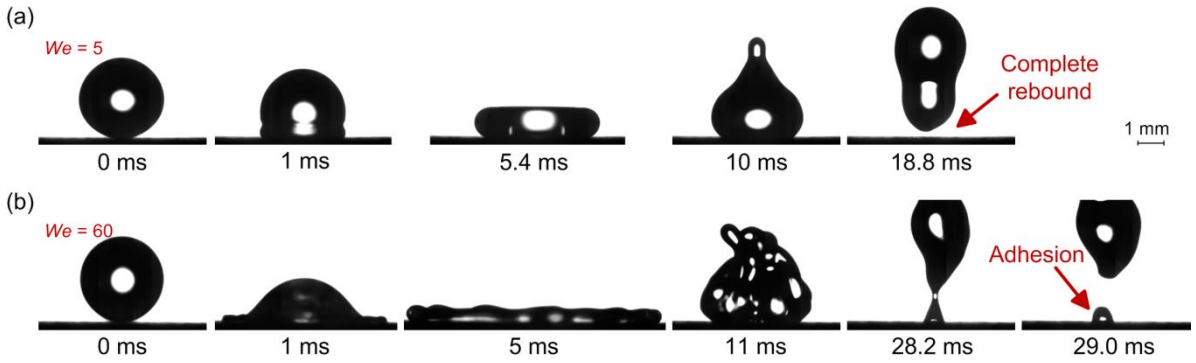

Fig. S5. Drops mimicking the super-cooled water (40 wt% glycerol in water) impacting on the passive porous superhydrophobic surface (P = 0 kPa). (a) We = 5 and (b) We = 60. On the passive superhydrophobic surface, at We = 5, the drop rebounded at 18.8 ms following the conventional rebound pathway (spreading, retracting, and rebounding); at We = 60, drop adhesion was observed. Drop diameter: 3.28 mm.

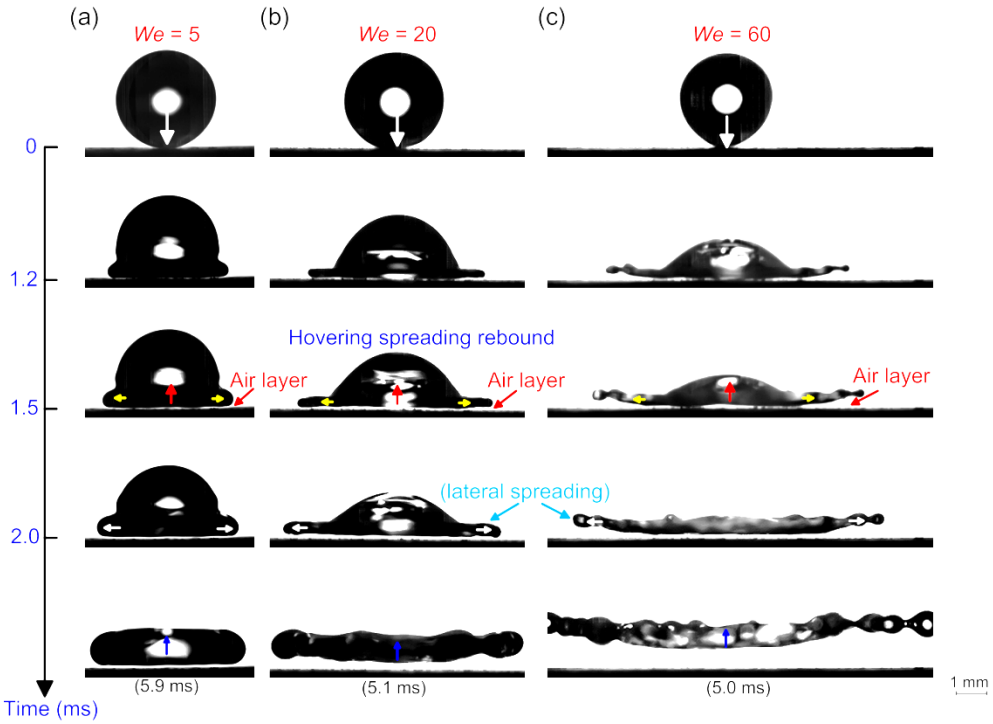

Fig. S6. Hovering spreading rebound for drops mimicking the super-cooled water (40 wt% glycerol in water) on the porous superhydrophobic surface with active air plastron (P = 200 kPa). (a) We = 5, (b) We = 20 and (c) We = 60 (Movie S4, ESI†). Hovering spreading rebound was robustly observed around 1.5 ms at both small and high We numbers for the 40 wt% glycerol in water. Drop diameter: 3.28 mm.

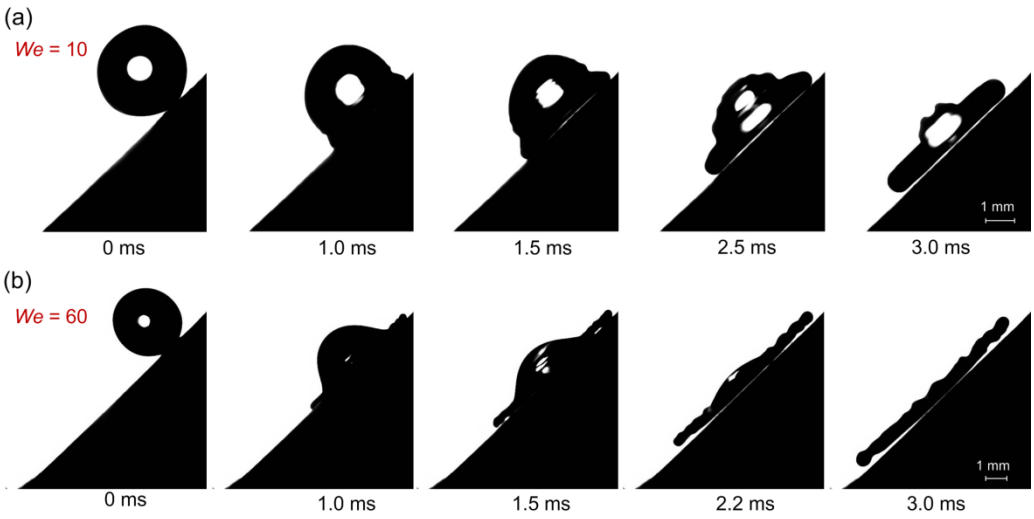

Fig. S7. Snap shots showing the hovering spreading rebound of water drops impacting on the tilted SHP surface with low pressure active air plastron (P = 100 kPa). (a) We = 10 and (b) We = 60. Tilt angle: 45°; diameter of the water drop: 3.04 mm.

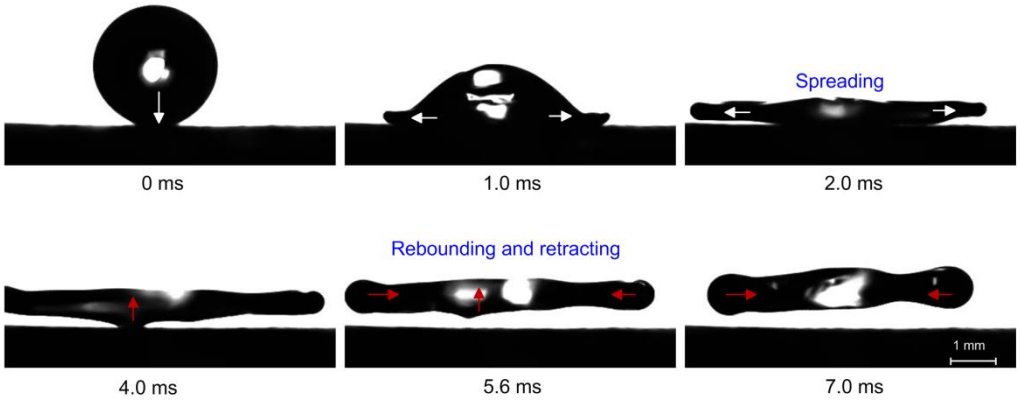

Fig. S8. Snap shots showing the rebounding of a 90 wt% glycerol drop on the porous superhydrophobic surface with low pressure air plastron (P = 100 kPa) at We = 60. Drop diameter: 2.75 mm.

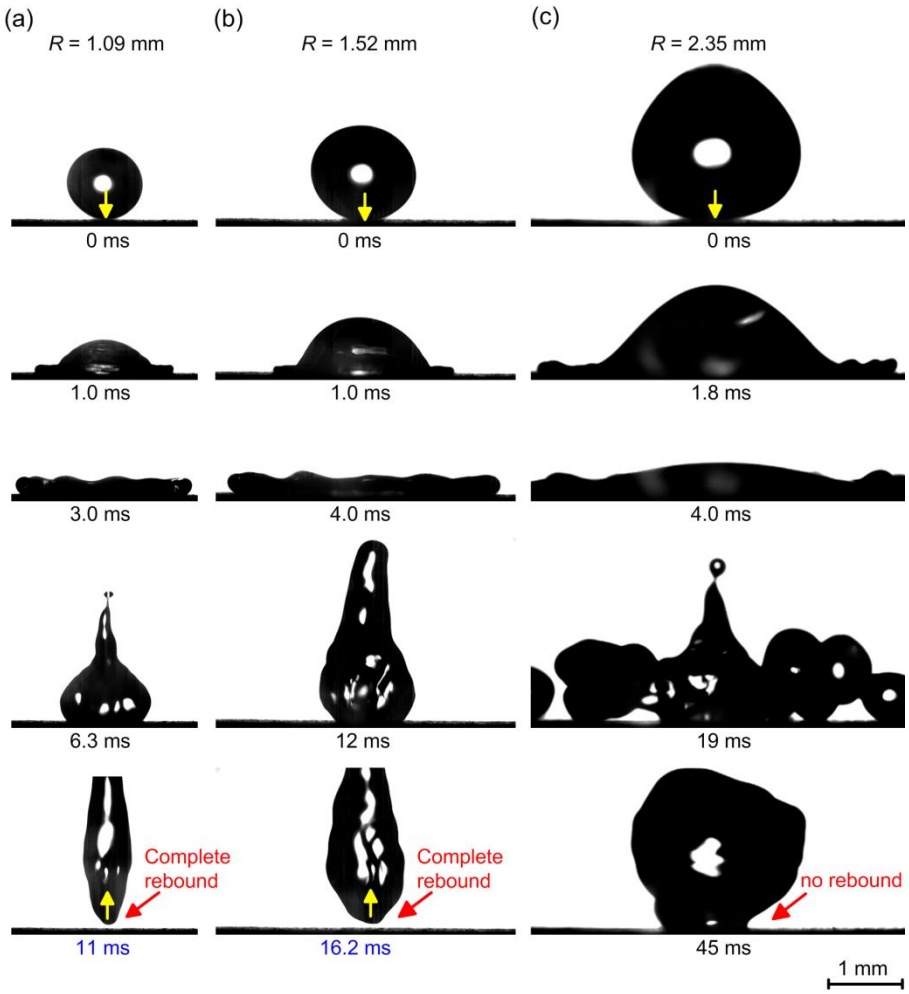

Fig. S9. Impacting dynamics for water drops of different radius on the passive porous superhydrophobic surface. Rebound time is found to be affected by drop size, with small drops having a lower contact time. When the drop diameter is too large (for instance R = 2.35 mm), the drop would adhere on the passive superhydrophobic surface and not rebound as shown in c. Drops were released from the same height H = 80 mm.

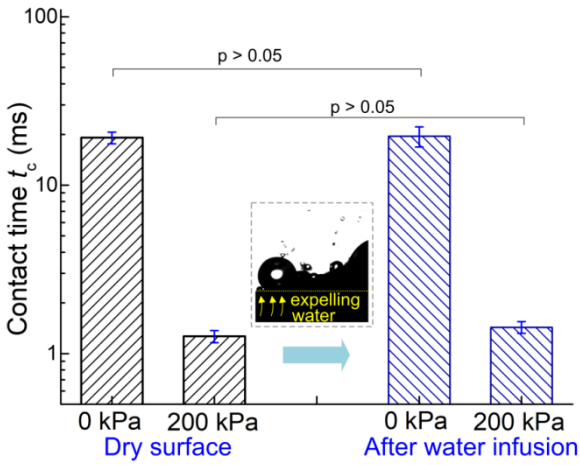

Fig. S10. *In-situ* restoration of the Cassie-Baxter state. The porous superhydrophobic surface was wetted by infusing water through its porous medium; after water invasion, the surface become hydrophilic. Moisture within the porous mediums was subsequently expelled by applying the active air plastron. Drop impacting tests were performed (diameter of the water drop: 3.04 mm; pressure: 0 kPa or 200 kPa) to compare the contact time before and after water invasion (n = 3). P values are determined by a Student's t-test. It shows that the superhydrophobic surface after water invasion has the same rebounding dynamics as its dry counterpart, demonstrating that the high pressure active air plastron can help restore the superhydrophobicity *in situ*.

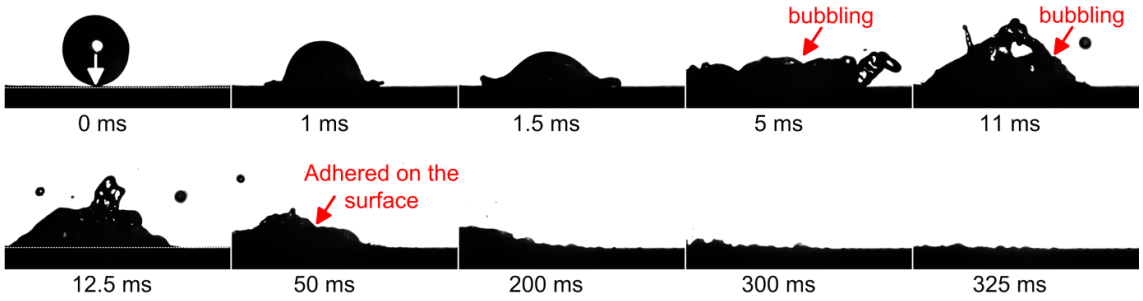

Fig. S11. A water drop impacting on the porous hydrophilic surface (*P* = 200 kPa, *We* = 30, water drop diameter: 3.04 mm). The porous hydrophilic surface was prepared by treating the porous superhydrophobic surface by oxygen plasma for 10 minutes at 150 W (model ATTo, Diener Electronic, Germany).[1] After oxygen plasma treatment, the surface became superhydrophilic; the water droplet quickly absorbed into the porous medium with a water contact angle of nearly 0°. The impinging water drop was adhered on the porous hydrophilic surface and did not rebound, showing that hovering spreading rebound would be synergic effect of both the superhydrophobicity and high pressure active air plastron.

Table S1. Contact time of bouncing drops reported in the literature

References	Liquid	Contact time t_c (ms)	Dimensionless contact time (t_c/τ)
Bird et al., Nature, 2013[2]	Water	7.8	1.4
Liu et al., Nature Physics, 2014[3]	Water	3.4	0.53
Gauthier et al., Nature Communication, 2015[4]	Water	7.6	1.38
Liu et al., Nature communication, 2015[5]	Water	10.3	1.59
Weisensee et al., Scientific reports, 2016[6]	Water	4	2.06
Song et al., ACS Nano, 2017[7]	Water	8.3	1.1
Graeber et al., Applied Surface & interface, 2018[8]	Water, glycerol	3.4	0.8
Zhan et al., Physical Review Letters, 2021[9]	Water	13.7	0.67
Hu et al., Langmuir, 2022[10]	Water	11.2	0.64
Qian et al., Advanced Science, 2022[11]	Water	2.9	0.504
This study	Water, glycerol	**~ 1.2**	**0.17**

Note: Representative studies published before 2013 can be found in Extended Table 1 from Ref 2.

Table S2. Physical properties of the water glycerol mixture[12]

Glycerol weight percentage (wt%)	Density (kg m^{-3})	Surface tension (mN m^{-1})	Dynamic viscosity (mPa s)	Drop diameter (mm)
0	998	72	1.005	3.04
10	1021	70.5	1.31	2.93
20	1045	69.5	1.76	3.53
30	1071	68.5	2.5	3.45
40	1098	67.9	3.72	3.28
50	1125	67.4	6	3.09
60	1153	66.9	10.8	3.07
70	1181	66.5	22.5	2.96
80	1209	65.7	60.1	2.86
90	1235	64.5	219	2.75

Description of Supplementary Movies

Movie S1.

A water drop impacting on the passive SHP surface (P = 0 kPa, We = 10).

Movie S2.

A water drop impacting on the active SHP surface (P = 200 kPa, We = 10).

Movie S3.

A water drop impacting on the active SHP surface (P = 200 kPa, We = 60).

Movie S4.

A 40 wt% glycerol drop impacting on the active SHP surface (P = 200 kPa, We = 60).

Movie S5.

A water drop impacting on the inclined passive SHP surface (P = 0 kPa, We = 10).

Movie S6.

A water drop impacting on the inclined active SHP surface (P = 200 kPa, We = 30).

Movie S7.

A 90 wt% glycerol drop impacting on the active SHP surface (P = 200 kPa, We = 10).

Movie S8.

A 90 wt% glycerol drop impacting on the active SHP surface (P = 200 kPa, We = 60).

Movie S9.

Water drops of different radius impacting on the active SHP surface (P = 200 kPa, H = 80 mm).

References

1 D. Mitra, M. Li, E. T. Kang and K. G. Neoh, *ACS Appl. Mater. Inter.*, 2019, **11**, 73-83.

2 J. C. Bird, R. Dhiman, H. M. Kwon and K. K. Varanasi, *Nature*, 2013, **503**, 385.

3 Y. H. Liu, L. Moevius, X. P. Xu, T. Z. Qian, J. M. Yeomans and Z. K. Wang, *Nat. Phys.*, 2014, **10**, 515-519.

4 A. Gauthier, S. Symon, C. Clanet and D. Quéré, *Nat. Commun.*, 2015, **6**, 8001.

5 Y. Liu, M. Andrew, J. Li, J. M. Yeomans and Z. Wang, *Nat. Commun.*, 2015, **6**, 10034.

6 P. B. Weisensee, J. Tian, N. Miljkovic and W. P. King, *Sci. Rep.*, 2016, **6**, 30328.

7 J. L. Song, M. Q. Gao, C. L. Zhao, Y. Lu, L. Huang, X. Liu, C. J. Carmalt, X. Deng and I. P. Parkin, *ACS Nano*, 2017, **11**, 9259-9267.

8 G. Graeber, O. B. Martin Kieliger, T. M. Schutzius and D. Poulikakos, *ACS Appl. Mater. Inter.*, 2018, **10**, 43275-43281.

9 H. Y. Zhan, C. G. Lu, C. Liu, Z. A. K. Wang, C. J. Lv and Y. H. Liu, *Phys. Rev. Lett.*, 2021, **126**, 234503.

10 Z. Hu, F. Chu, Y. Lin and X. Wu, *Langmuir.*, 2022, **38**, 1540-1549.

11 C. L. Qian, F. Zhou, T. Wang, Q. Li, D. H. Hu, X. M. Chen and Z. K. Wang, *Adv. Sci.*, 2022, e2103834.

12 G. Graeber, O. B. Martin Kieliger, T. M. Schutzius and D. Poulikakos, *ACS Appl. Mater. Inter.*, 2018, **10**, 43275-43281.